

A High- T_c Superconductor Bolometer for Remote Sensing of Atmospheric OH

M.J.M.E. de Nivelles, M.P. Bruijn, M. Frericks, R. de Vries, J.J. Wijnbergen, P.A.J. de Korte, S. Sánchez*, M. Elwenspoek*, T. Heidenblut**, B. Schwierzi**, W. Michalke*** and E. Steinbeiss***

Space Research Organization Netherlands, Sorbonnelaan 2, 3584 CA Utrecht, The Netherlands

** MESA Research Institute, P.O. Box 217, 7500 AE Enschede, The Netherlands*

*** Institut für Halbleitertechnologie und Werkstoffe der Electrotechnik, Universität Hannover, 30167 Hannover, Germany*

**** Institut für Physikalische Hochtechnologie, Helmholtzweg 4, 07743 Jena, Germany*

Abstract. The technological feasibility is being investigated of a high- T_c superconductor transition edge bolometer for far-infrared detection, which can meet the requirements of a Fabry-Perot based satellite instrument designed for remote sensing of atmospheric OH. These include a time constant $\tau < 0.3$ s, an operating temperature above 35 K, a diameter of 1.1 mm, and a noise equivalent power (NEP) smaller than about $4.0 \cdot 10^{-12}$ W Hz^{-1/2} for radiation with $\lambda = 85$ μ m. Presently, no other sensor can meet these requirements.

A NEP value of $3 \cdot 10^{-11}$ W/Hz^{1/2} and $\tau = 0.4$ ms has been realized with high- T_c bolometers on Si membranes with a receiving area of 0.85×0.85 mm². By replacing the Si by Si₃N₄ we expect that the thermal conductance G can be reduced by more than a factor 20. This should result in a NEP less than $4 \cdot 10^{-12}$ W/Hz^{1/2} and a time constant < 0.1 s.

A bond-and-etch-back technique is used to prepare a mono crystalline silicon top layer on the Si₃N₄ membrane, which is necessary for the epitaxial growth of the superconductor. An absorption layer will be added to the detector to enhance the efficiency. Promising candidates for use as an absorption layer are metal black films with an efficiency η around 80% at 85 μ m wavelength.

1. INTRODUCTION

In the context of the PIRAMHYD program (Passive Infra-Red Atmospheric Measurements of HYDdroxyl) of the European Space Agency (ESA) we are investigating the fabrication of a high- T_c superconductor transition edge bolometer.

The PIRAMHYD program aims at the global monitoring of important species in the atmospheric chemistry by limb sounding of self-emitted radiation. Hydroxyl has the first priority because of its central importance in stratospheric chemistry and the lack of data on its concentration. A few different measurement techniques are being investigated, i.e. a Fourier transform spectrometer, a heterodyne receiver and the OH Interferometer Observations (OHIO) instrument.

The OHIO instrument includes a Fabry-Perot and reflection grating for selection of the 84.42 μ m emission line of OH [1]. The observation time, the OH line intensity, the throughput and transmission of the Fabry-Perot and the necessary Signal-to-Noise ratio dictate the detector requirements: i.e. a diameter of 1.1 mm, a time constant less than 0.3 s and a Noise Equivalent Power (NEP) better than $4.0 \cdot 10^{-12}$ W/Hz. To increase operation time the instrument is designed for cooling by a mechanical cryocooler. This requires an operational temperature of the detector larger than 35 K.

For wavelengths < 20 μ m liquid nitrogen cooled photodetectors like HgCdTe can be used, but for longer wavelengths and temperatures above 35 K none of the presently available detectors can meet the requirements. Most promising are bolometers with a high- T_c superconductor transition edge thermometer [2].

Recently we reported on high- T_c GdBa₂Cu₃O_{7- δ} transition edge bolometers on micromachined silicon membranes with an operating temperature of about 85 K [3]. For the fabrication an epitaxial YSZ+CeO₂ buffer layer and an inhibition patterning technique were used. However, due to the high thermal conductance of the silicon membrane, the sensitivity is too small for the OHIO instrument. A calculation of the

thermal conduction noise shows that the NEP requirement imposes an upper limit on the thermal conductance G of about $3 \cdot 10^{-5}$ W/K. In order to realize this value we aim at the replacement of the silicon by silicon nitride which has a much smaller thermal conductivity.

At $85 \mu\text{m}$ wavelength the reflectivity of $\text{GdBa}_2\text{Cu}_3\text{O}_{7.8}$ is almost 100%. To improve the efficiency in the far infrared an absorption layer will be added to the design. We will investigate different options like gold- or silver blacks and thin resistive metallic layers.

In this presentation we discuss the preparation technology, the first results and the expected performance of the Si_3N_4 membrane bolometers.

2. PREPARATION TECHNOLOGY

Analysis of available data on the $1/f$ -voltage noise of high- T_c films shows that its contribution to the NEP of the detector remains within the requirements, provided that the superconducting film is of good epitaxial quality [4]. To enable epitaxial growth of the superconductor, a single crystalline Si layer is required on top of the Si_3N_4 membrane. A cross section of the obtained multilayer structure is shown in Fig. 1. Here we will focus on the preparation of the Si_3N_4 membranes with a single crystalline Si top layer, which is a technological key issue in the production process. For the deposition of the YSZ/ CeO_2 bufferlayer, the preparation of the inhibition pattern, the growth of the high- T_c superconductor, the deposition of the PtO_x passivation layer and the laser writing of the Pt contacts, we refer to [3].

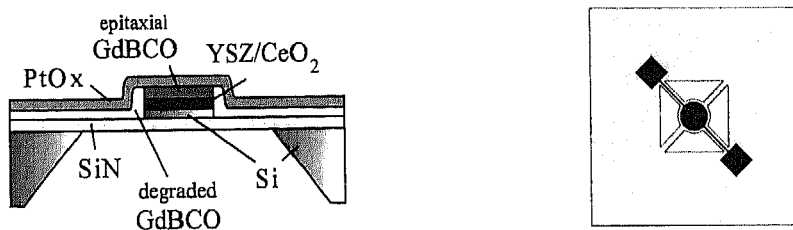


Figure 1: Cross section and top view and of the high- T_c bolometer

2.1 Bond-And-Etch-Back Technologies

For the production of the $\text{Si}_3\text{N}_4/\text{Si}$ bilayer two bond-and-etch-back technologies are being investigated, both involving a silicon fusion bonding step between Si_3N_4 and Si. The first route involves the use of a high concentration boron layer, which can be used as an etch stop in KOH/IPA (IsoPropyl Alcohol). The second route involves the use of a SOI wafer. By transferring the thin silicon top layer to the nitride wafer it should be possible to obtain the $\text{Si}_3\text{N}_4/\text{Si}$ layer. The process schemes are shown in Fig. 2.

In initial bonding experiments it was found that both low stress Si_3N_4 (> 400 nm thick) as well as high boron doped surfaces (from a solid source dotation system) are too rough

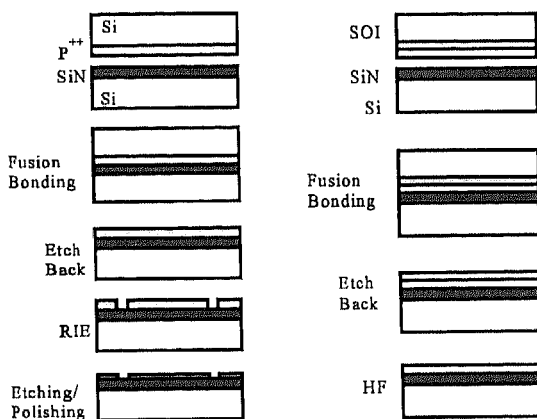


Figure 2: Process schemes for routes 1 (left) and 2 (right)

for fusion bonding. In literature successful bonding results between Si and Si_3N_4 have been mentioned [5,6], but these involved Si_3N_4 layers with a thickness of 300 nm or less. It was found that by using a

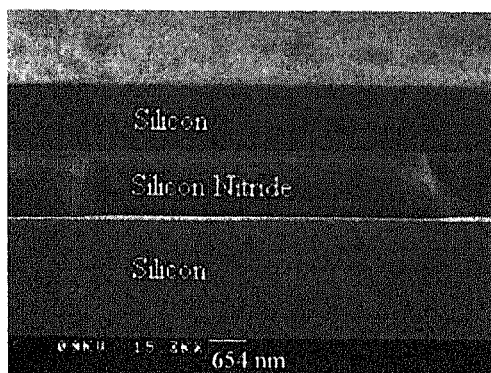


Figure 3: Cross section of Si-Si₃N₄ layer from the SSD wafer after bond-and-etch-back.

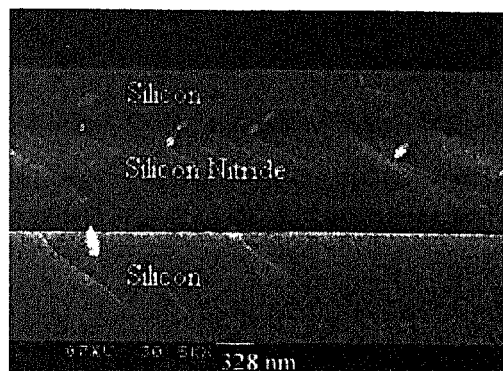


Figure 4: Cross section of Si-Si₃N₄ layer from the implanted wafer after bond-and-etch-back.

Chemical Mechanical Polishing (CMP) step, previously unbondable Si₃N₄ and boron doped surfaces became bondable [7]. After bonding, the Si wafer is etched back until the etch stop is reached.

2.2 Experimental

In recent bond-and-etch-back experiments for route 1, 380 μm thick 3" (100) p-type wafers were used. On three wafers a 1.1 μm thick low-stress LPCVD Si₃N₄ layer was grown. Boron doping was done with both implantation and solid source dotation (SSD). Implantation was done at 200 keV, with a concentration of $2 \cdot 10^{16} \text{ cm}^{-2}$. A 30 min anneal at 960° C resulted in a doping profile with a maximum of about $1 \cdot 10^{20} \text{ cm}^{-3}$ at a depth of 1 μm . One implanted wafers was polished before further processing, and one wafer was used unpolished. Doping in the SSD system left a surface boron concentration of about $3 \cdot 10^{20} \text{ cm}^{-3}$ and a depth of 2.1 μm . This wafer was polished before further processing.

Prior to bonding the wafers were given a standard clean, using fuming nitric acid (100%) and hot nitric acid (70%, 90° C). An IR camera was used to monitor the initial bonding of the wafers. By gently pressing the wafers together in the center with a tweezer, the wafers were brought into close contact.

It was found that the unpolished implanted wafer bonded spontaneously, immediately after getting in close contact. A complete bond was reached within 2 seconds, with only one void. The polished implanted wafer bonded very bad. After continuously pressing, only a few parts remained bonded. The SSD wafer did not bond spontaneous, but after pressing some more, a complete bond was achieved. After the prebond the wafers were annealed for 2 hours at 900° C in N₂.

Etching back was carried out in a two-step process. First, a 25 wt% KOH solution at 77° C was used to etch the bulk silicon until about 40-60 μm was left. Then a mixture of KOH (23.4 wt%), IPA (13.3 wt%) and H₂O (63.3 wt%) at 80° C was used to remove the remaining silicon, and stop at the high doped boron layer. During etching, the unbonded parts of the badly bonded wafer pair came off, leaving about 10% of the surface covered with silicon. On the other two wafers about 90% remained covered with Si. After etching back and stopping at the high concentration boron layer, a thin silicon layer remained on top of the Si₃N₄. The thickness of this layer was 1.1 μm in case of the SSD wafer (Fig. 3) and 0.4 μm in case of the implanted wafer (Fig. 4).

The bond-and-etch-back procedure still has to be optimized. The main problems are hillock formation during etching in the KOH/IPA system, and small holes which are revealed in the thin Si top layer after etching back. The presence of IPA enhances the hillock formation, since after etching in just KOH no hillocks were visible. Adjusting the concentrations and temperature should strongly reduce the amount and size of the hillocks. The holes are believed to be the result from small air bubbles which are a product from the chemical reaction that takes place at the bonded interface during the annealing step.

These bubbles have not disappeared because of the rather low annealing temperature. At temperatures

above 1000° C these bubbles should disappear, but at this temperature the concentration profile of the implanted wafers will change significantly.

In route 2 the etch stop is provided by the buried oxide (BOX) layer from the SOI wafer. So the thin silicon layer is still unaffected by etching back the bulk of the SOI wafer. Removing the oxide layer with buffered HF finally leaves the thin silicon layer on top of the silicon nitride. The advantage of route 2 is that by using SOI wafers with a Si top layer of several hundred nm only a small amount of Si has to be removed by either polishing or etching to obtain the required thickness. Experiments for route 2 will be carried out in the near future.

3. PERFORMANCE MODELLING

3.1 Thermal response

Although we aim at a bolometer which is suspended by small Si_3N_4 beams the first examples will be on closed membranes. To estimate the thermal response of such bolometers we have used a simple numerical model describing the heating of the membrane and the corresponding resistance change of the high- T_c thermometer. For simplicity and to speed up simulations the actual membrane is approximated by a circular shape. The diameter is chosen such that the detector area is conserved. The resistance of the transition edge thermometer is modelled by series connection of annular rings of high- T_c film, coaxial on the membrane. The resistance is a linear function of the temperature (for small ΔT). Similar simulations have been described by Fenner et al. [8].

First we modelled the Si-membrane bolometers. They consist of a 1 μm Si membrane, a 50 nm

Table 1: Thermal properties of bolometer materials at 90 K (From [9,10,11,12]). * κ of Si_3N_4 is calculated from the data in [13].

material	κ (W/cmK)	c (W/cm ³ K)
Si ([B]= $3 \cdot 10^{20}$ cm ⁻³)	0.5	0.52
Si_3N_4	0.012*	0.31
YSZ/CeO ₂	0.015	0.7
GdBa ₂ Cu ₃ O _{7-δ} (<i>ab</i> -plane)	0.085	1.1

YSZ/CeO₂ bufferlayer, a 50 nm GdBa₂Cu₃O_{7- δ} high- T_c film, and a 100 nm PtO_x passivation layer. For the thermal properties the values listed in Table 1 have been used. Assuming a negligible contribution from the PtO_x passivation layer, the average thermal conductivity becomes $\kappa=0.42$ W/cmK and the average heat capacity $c=0.57$ J/cm³K. Both values are dominated by the properties of the Si membrane. Putting these values into the simulations we found $G=7 \cdot 10^{-4}$ W/K and $\tau=6 \cdot 10^{-4}$ s, close to the actually measured values of $G=4.5 \cdot 10^{-4}$ W/K and $\tau=4 \cdot 10^{-4}$ s [3].

In the Si_3N_4 membrane bolometers most of the Si is replaced by Si_3N_4 . By using inhibition structuring [3] the single crystalline silicon top layer of approximately 200 nm is only present at the location of the high- T_c meander. The average κ and c in the central part of the membrane with $r < r_1$, can be estimated to be 0.08 W/cmK and 0.4 J/cm³K, respectively. Outside the region of the meander ($r > r_1$) κ and c are 0.02 W/cmK and 0.4 J/cm³K. The radiation is focused and absorbed homogeneously in the area with $r < r_2$, and the perimeter of the membrane is r_3 . Fig. 5 shows an example of a calculated temperature profile and the corresponding step response of the resistance. In Table 2 the resulting G and τ are listed for different r_3/r_2 , with $r_2=0.55$ mm (detector requirement) and $r_1=0.8$ r_2 . In addition the values of G' and τ' are added, which are the corrected values of G and τ for the heat conductance due to the contact leads.

A further reduction of G is possible by etching windows in the Si_3N_4 membrane. In the optimum situation the central region of the bolometer ($r < r_2$) is suspended by small Si_3N_4 beams. This detector can simply be modelled as a heatcapacitance C equal to the heatcapacitance of central region of the bolometer, connected to the heatsink via a thermal conductance G , equal to the heat conductance of the beams

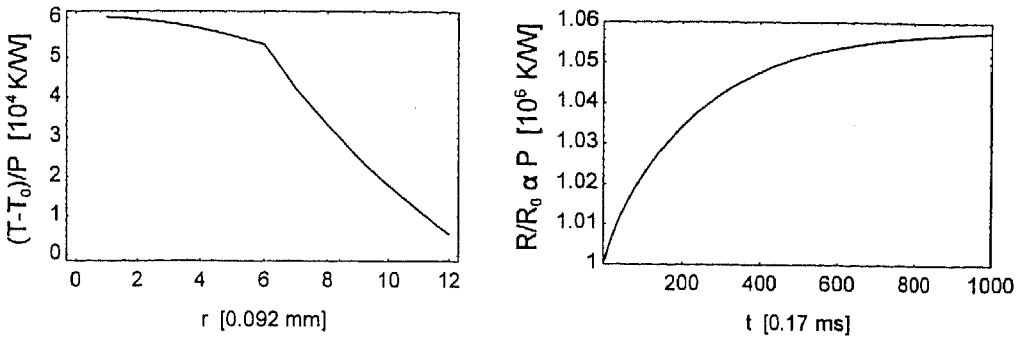


Figure 5: Steady state temperature profile and step response of a ring model bolometer on a Si_3N_4 membrane ($r_3/r_2=2$, $\tau_2=0.55$ mm).

(including the contact leads). In case of 4 beams with each a length 0.5 mm and width 0.2 mm, the estimated G equals $8 \cdot 10^{-6}$ W/K (including silicon along contact leads), $C_e=6 \cdot 10^{-6}$ J/K (including silver black absorber) and $\tau=0.07$ s.

Table 2: G , τ and NEP of the SiN_x membrane bolometer as determined from the numerical simulations. G' and τ' are the corrected values of G and τ due to the heat conductance of the contact leads with a total width of 0.2 mm. C_e is the effective heat capacity $G'\tau'$ bolometer suspended by 4 legs as described in the text.

r_3/r_2	G (W/K)	τ (s)	G' (W/K)	τ' (s)	C_e (J/K)	NEP _{phonon} (W/ $\sqrt{\text{Hz}}$)	NEP _{excess} (W/ $\sqrt{\text{Hz}}$)	NEP _{total} (W/ $\sqrt{\text{Hz}}$)
1.5	$2.5 \cdot 10^{-5}$	0.023	$3.3 \cdot 10^{-5}$	0.017	$6 \cdot 10^{-7}$	$4.3 \cdot 10^{-12}$	$2.1 \cdot 10^{-12}$	$4.8 \cdot 10^{-12}$
2	$1.7 \cdot 10^{-5}$	0.042	$2.1 \cdot 10^{-5}$	0.034	$7 \cdot 10^{-7}$	$3.4 \cdot 10^{-12}$	$1.9 \cdot 10^{-12}$	$3.9 \cdot 10^{-12}$
3	$1.2 \cdot 10^{-5}$	0.010	$1.4 \cdot 10^{-5}$	0.085	$1.2 \cdot 10^{-6}$	$2.8 \cdot 10^{-12}$	$2.0 \cdot 10^{-12}$	$3.4 \cdot 10^{-12}$
2*			$8 \cdot 10^{-6}$	0.07	$6 \cdot 10^{-7}$	$2.1 \cdot 10^{-12}$	$1.0 \cdot 10^{-12}$	$2.3 \cdot 10^{-12}$

3.2 Absorption efficiency

The measured absorption efficiency η of the silicon membrane bolometer in the infrared is only 0.13 at $\lambda=13 \mu\text{m}$ and 0.16 at $\lambda=6 \mu\text{m}$ [3]. At $85 \mu\text{m}$ an absorptance around 10 % has been predicted [14]. Although less important if the bolometer is mounted in an optical cavity, an absorption layer is required for good performance. Among the most promising absorption layers for use in the far infrared are metal blacks. An absorptance η of 0.8 at $\lambda=85 \mu\text{m}$ was measured for a $6.2 \mu\text{m}$ Ag-vacuum mixture with a filling percentage of 1% [15]. The additional heat capacitance of such a layer deposited on the receiving area of the bolometer is about $1 \cdot 10^{-7}$ J/K. This corresponds with a relative increase of the effective heatcapacity and the bolometer time constant (Table 2) of only 9 to 16%.

3.3 Noise calculations

A calculation of the detector NEP of the Si_3N_4 membrane bolometer (with typical parameters $T_c=80$ K, $R=5$ k Ω , $\alpha=1$ K $^{-1}$ [3], and G and τ as listed in Table 2) shows that the most fundamental and important contributions to the detector noise are the phonon noise (i.e. the noise related to the thermal conductance G), and the excess noise in the high- T_c film. Thermal fluctuation noise and amplifier noise can be reduced sufficiently by using a suitable biasing scheme, e.g. a bridge configuration with ac bias current and a low noise amplifier. The Johnson noise and the background radiation noise are negligible. In Table 2 the phonon NEP= $\sqrt{(4kT^2G'/\eta^2)}$ is listed for $T=80$ K and $\eta=0.8$.

The excess noise of the superconducting thermometer depends strongly on the structural quality of the high- T_c material. Analysis of various noise measurements showed us that at the midpoint of the superconducting transition the excess noise of epitaxial $\text{YBa}_2\text{Cu}_3\text{O}_{7-x}$ can be estimated from the Hooje

law $S_v(f)/V^2 = \gamma/(n_c E f)$, with $S_v^{1/2}(f)$ the voltage noise spectral density, V the voltage, γ a dimensionless constant, n_c the charge carrier density and f the frequency [4]. An average value $\gamma/n_c = 5 \cdot 10^{-22} \text{ cm}^3$ was found. The volume E of the meandered high- T_c film is approximately $2 \cdot 10^{-8} \text{ cm}^3$. The NEP can be calculated by substituting the Hooge law into $\text{NEP}_{\text{excess}} = S_v^{1/2}/|S|$, with $|S| = \eta IR \alpha / G_e |1 + i2\pi f \tau_e|$ the bolometer responsivity. G_e is the effective thermal conductance with the thermal feedback due to the bias current heating taken into account and τ_e is the corresponding effective time constant. Typically, G_e is 0.7 times the heat conductance G . Minimizing the NEP with respect to signal modulation frequency f yields an optimum f of $1/2\pi\tau_e$. The resulting $\text{NEP}_{\text{excess}}$ is shown in Table 2 for the given values of G' and τ' and $\eta=0.8$.

The last column shows the total NEP due to both phonon and excess noise. The required NEP is realized for the last three options, with the lowest NEP for a structured membrane.

4. CONCLUSIONS

It is expected that with a combination of $\text{Si}_3\text{N}_4/\text{Si}$ membrane fabrication and existing technologies as presented in [3] high- T_c bolometers can be made with the required specifications. The proposed routes for the production of the $\text{Si}_3\text{N}_4/\text{Si}$ layers and membranes are still under investigation. The main points of attention at this moment are to increase the bonding yield, and achieve an etched-back surface without hillocks. The combination of micromachining and superconductive films provides an interesting challenge, leading to new possibilities for the development of far infrared detectors with unequalled performance at temperatures around 80 K.

Acknowledgments

The authors would like to thank C. Gui for carrying out the CMP experiments. This project funded by the European Space Agency under contract no. 11738/95/NL/PB (project manager Dr. E. Armandillo).

References

- [1] Wijnbergen J.J., de Korte P.A.J., de Nivelles M.J.M.E., *Proc. SPIE* **2578** (1995) 306.
- [2] Richards P.L. et al., *Appl. Phys. Lett.* **54** (1989) 283-285.
- [3] Neff H., Laukemper J., Khrebtov I.A., Tkachenko A.D., Steinbeiss E., Michalke W., Burnus M., Heidenblut T., Hefle G. and Schwierzi B., *Appl. Phys. Lett.* **66** (1995) 2421-2423.
- [4] de Korte P.A.J., de Nivelles M.J.M.E., Wijnbergen J.J., *Proc. SPIE* **2578** (1995) 294.
- [5] Bower R.W., Ismail M.S., Roberts B.E., *Appl. Phys. Lett.* **62** (1993) 3485.
- [6] Harendt C., Graf H.-G., Höfflinger B., Penteker E., *J. Micromech. Microeng.* **2** (1992) 113.
- [7] Gui C., Gardeniers J.G.E., Elwenspoek M., Albers H., Lambeck P.V., "Silicon fusion bonding with chemical mechanical polishing", *Sensor Conf.*, Delft (The Netherlands) 20-21 March, 1996.
- [8] Fenner D.B., Li Q., Hamblen W.D., Luo J., and Hamblen D.G., *Proc. SPIE* **2159** (1994) 10-20.
- [9] Touloukian Y.S., *Thermophysical properties of Matter Vol. 2 and 5* (Plenum, New York, 1970).
- [10] Verghese S., *Infrared detection with high- T_c bolometers and response of Nb tunnel junctions to picosecond voltage pulses* (PhD thesis, University of California at Berkeley, 1993).
- [11] Inderhees S.E. et al., *Phys. Rev. Lett.* **66** (1991) 232-235.
- [12] Hagen S.J., Wang Z.Z. and Ong N.P., *Phys. Rev. B* **40** (1989) 9389-9392.
- [13] Johnson B.R., Foote M.C., Marsh H.A. and Hunt D.B., *Proc. SPIE* **2267** (1994).
- [14] Zhang Z.M. and Flik M.I., *IEEE Trans. Appl. Superc.* **3** (1993) 1604-1607.
- [15] Neff H., Henkel S., Sass J.K., Steinbeiss E., Ratz P., Müller J. and Michalke W., "Optical properties of ultrathin silver films on silicon", submitted to *J. Appl. Phys.*